Two-temperature-region model for cluster-growth simulations: Formulation and application to the growth of fcc 201-atom Lennard-Jones clusters

W. Polak
Department of Applied Physics, Institute of Physics, Lublin University of Technology, ulica Nadbystrzycka 38, 20-618 Lublin, Poland
(Received 18 May 2004; revised manuscript received 25 March 2005; published 22 June 2005)

The growth of Lennard-Jones clusters was simulated using a specially developed technique based on applying the Monte Carlo method and distinguishing two regions (nucleus and vapor) of two different temperatures. Cluster growth was initiated from a 201-atom cluster in the truncated octahedron form of initially perfect fcc structure and ended when the cluster was composed of ca. 2000 atoms. Three reduced temperatures $T_n^*=0.25$, 0.30, and 0.35 as well as four different atom concentrations in the vapor region were analyzed to find parameters enabling a good atom ordering in the growing cluster. The simulations revealed that at sufficiently slow growth the clusters are very well arranged with the order parameter in the range from 91% to 98% depending on the temperature. However, all growth simulations always lead to the formation of hcp planes on some (111) dense-packed cluster planes due to a misfit in the position of newly added atoms resulting in …*ABCABA* instead of …*ABCABC* layer sequence. The subsequent growth of the created hcp layer can lead to the enlargement of this layer or to the formation of an fcc plane over the existing hcp one in the process of kinetic trapping. As observed in the simulations, two hcp planes crossing at an angle close to 70.53° usually form a linear chain of decahedral local structures in the contact region. This mechanism transforms a defected crystalline cluster to a noncrystalline one.

DOI: 10.1103/PhysRevB.71.235413 PACS number(s): 61.46.+w, 61.72.Nn, 02.70.Uu, 81.10.Aj

I. INTRODUCTION

Clusters, as very small parts of a material, have properties different from those of bulk material. One of them is their structure, which is widely believed to change always with growing cluster size from a noncrystalline to crystalline structure. In the case of some substances, such a structural transition occurs at a sufficiently small cluster size and can be found relatively easily in experiments with cluster beams (e.g., CO_2 clusters[1]) or in computations (e.g., NaCl clusters[2]). However, clusters of many different substances are predicted to show crystalline structure at relatively large sizes,[3,4] where experimental data analysis is not easy and conclusions are not clear. Since some of such clusters are in the reach of the growing calculation possibilities of modern computers, the importance of theoretical methods has increased tremendously in recent years. For example, it was possible to obtain more detailed information on the mechanism of structure formation during simulated growth of large silver and gold clusters composed of $N=1289$ atoms.[5]

Investigation of cluster structure gives unclear results in the case of the model material: the heavier rare-gas elements (Ar, Ne, Kr, Xe). Experimental results derived from electron diffraction on Ar cluster beams[6,7] reveal that defective clusters dominate the cluster spectrum up to $N=10^5$ and there is no sign of attaining bulk structural properties. However, apart from the statement that clusters are composed of face-centered-cubic (fcc) and the hexagonal-close-packed (hcp) mixed domains, no definite conclusion concerning the structure of these clusters was drawn[6,7] from the data analysis. This is partly due to unavoidable averaging over different cluster structures present in cluster beams. It is also due to a lack of theoretical models of atom arrangement in large clusters.

From a theoretical point of view, the van der Waals interatomic interaction between rare-gas atoms seems to be sufficiently described by the Lennard-Jones (LJ) potential, which is typically used in the literature. However, many theoretical attempts failed even in explaining why the bulk heavier rare-gas crystals (which are simpler case than large clusters) adopt the fcc structure during crystallization.[8] From the pioneering theoretical work of Kihara and Koba[9] it is known that the hcp crystal structure is more strongly bounded for the LJ potential than fcc (although the difference in the binding energy is merely 0.01%). This result was confirmed recently by Stillinger[10] at a much higher level of precision in calculations.

The disagreement between theoretical predictions and experimental observations, called the rare-gas solid (RGS) problem, still remains unsolved. Some authors believed that it is caused by an insufficient accuracy of the LJ potential applied in calculations. However, when different pair potentials, three-body interactions, or entropy effects are analyzed (see the literature, e.g., in Refs. 6 and 8), the higher binding energy for the hcp structure is also obtained. Some researchers made attempts to explain the RGS problem assuming that the experimental solid structure is formed due to some kinetics effects which lead to the formation of nonoptimal (from energetic point of view) fcc cluster structure during the initial stage of nucleation and clustering. Unfortunately, simulations of nucleations from the supercooled liquid[11] were not able to realize stable fcc growth. It may be caused by the absence of fcc growth promoting defects, e.g., two parallel linear defects of pentagonal symmetry proposed by van de Waal,[12] in the clusters. In this context, it is reasonable to simulate clustering also from vapor to observe defects formed and find those promising the fcc growth.

To the author's knowledge, growth simulations have not been carried out for medium-sized (limited here to $150<N$

<1000) and large (thousands of atoms) rare-gas clusters. It seems that medium-sized rare-gas clusters are of great importance for explaining transition size effects. The author's results[13] show that some clusters of $N \approx 200$ atoms are possible to attain the defective crystalline structure in the form of mixed fcc and hcp layers. On the other hand, Ikeshoji *et al.*[14] found in simulations of cluster solidification by freezing that some clusters with $N \approx 450$ exhibit fcc structural properties. However, nothing is known about the possibility of reported clusters to develop solely the fcc structure in simulated cluster growth. This is because Ikeshoji *et al.*[14] solidified LJ clusters by evaporative or thermostatic cooling, where the number of cluster atoms decreases or is constant. The unique and natural way to prove how atom addition acts on an existing structure is reliable simulations of cluster growth.

The first aim of this paper is to formulate a reliable model of cluster growth, based on the Monte Carlo (MC) method, which could be efficient in simulations of middle-sized and large clusters. The second aim is to apply the model to the LJ cluster immersed in the vapor in order to investigate the nontrivial problem: is it possible to grow a perfect fcc cluster when the seed cluster is defectless fcc? van de Waal[15,16] argued that perfect fcc rare-gas clusters and crystals would develop into fcc-hcp mixtures due to stacking faults inevitably present during growth, because the interaction energy in "wrong" and "right" atom positions is practically the same. In order to prove van de Waal's arguments and to find in simulations possible problems in fcc cluster growth, in this work it was decided to analyze the growth of solid LJ clusters until $N \approx 2000$ starting from the 201-atom cluster in the form of a truncated octahedron, which is presumed[17] to be the preferred structure for this cluster size at $T=0$. The internal structures of all final clusters for different temperatures and growth ratios were observed using the coordination polyhedron method[13] and visualization of a selected structure to find the phase transformation or formation of defects.

II. MODELING OF CLUSTER GROWTH

The common features of cluster growth simulations are an addition of atoms to the cluster accompanied with a cluster structure equilibration realized by MC or molecular dynamics (MD) methods. For comparison, the atom addition, certainly present in real conditions, is absent in the global optimization technique, which dominates in the literature; an excellent overview of different techniques for determining the lowest-energy configuration of LJ clusters was given by Wille.[18] Moreover, due to the well-known exponential increase in the number of local potential minima with cluster size N,[18,19] the global optimization technique is limited to investigations of small clusters. In this context, computer simulations are a unique technique, which enables analysis of kinetics effects for medium-sized and large clusters.

The cluster growth models[5,20–22] based on MD can be described briefly as follows. The atom to be added to a cluster is randomly located on a sphere centered around the cluster mass center. Then it is moved radially[22] or in a random direction[5] towards the growing cluster. The atom deposition increases the cluster temperature significantly[5] due to release of the atom-cluster interaction energy and the atom kinetic energy. Therefore, clusters are thermostatted to keep the temperature almost constant. In the model, it is possible to observe atom diffusion on the cluster surface or inside the cluster since positions of atoms change in real time as governed by the laws of motion present in MD.

Apart from problems of good thermostating in MD growth models, there is another problem arising in implementing the MD method to large systems with large scales of simulated system time.[23] As argued recently by van der Eerden,[11] the time step used in numerical solutions of the motion equation should be sufficiently small (ca. 0.01 ps) to enable atom translations of acceptable value (1%–10% of atom size) for thermal motions. This small value of the time step and possibilities of modern computers limit simulations of liquids and solids to a few thousands of atoms observed during a few ns.[11] The results of the Baletto group on the growth simulation of small clusters composed of a few to about 150 Ag atoms[20] or C_{60} molecules[21] show that experimental time scales are not reachable by present computational means, though they were able to observe Ag cluster growth during 3 μs at an atom deposition interval close to an experimental one.

A different situation is in case of the Monte Carlo method, which is based on the acceptance or rejection of randomly selected atom translation using the Metropolis criterion applied for a given system temperature T. The atom translations also must be sufficiently small (in this work ca. 15% of atom diameter) to lead to a reasonable acceptance ratio (typically 0.4–0.6). As a result, the computational times of both methods are usually comparable.[11] However, some large systems or time scales can be reached only in MC simulations.[23] Moreover, the MC method is better suited to control the system parameters such as temperature or pressure.

Proposed model

The growth of Lennard-Jones clusters from vapor is simulated here using a specially developed model, which enables random atom movement inside the vapor surrounding a central cluster (hereafter also called a nucleus), where atoms can be built in the cluster when they approach its surface. This is realized by applying a nonstandard MC method. The main modifications are (i) controlled atom addition (particle creation) to the vapor region and (ii) distinguished two regions, nucleus and vapor, of two different temperatures and atom translation steps. The details and arguments for these modifications are given after presentations of the standard part of the model.

There are many assumptions in the model, which are very well known from the literature. The atom-atom interaction energy was calculated from the 12-6 Lennard-Jones potential:

$$U(r) = 4\varepsilon\left[\left(\frac{\sigma}{r}\right)^{12} - \left(\frac{\sigma}{r}\right)^{6}\right], \tag{1}$$

with the truncation distance $r_{tr}=3.4\sigma$.[13] As is typical for theoretical treatments, the potential parameters σ and ε are used

in this paper as the units of length and energy, respectively. Also the reduced temperature T^*, defined as $T^*=k_BT/\varepsilon$ with k_B representing the Boltzmann constant, was used instead of the absolute temperature T. In order to obtain real values of the parameters, e.g., for argon, one can use parameters given by Kittel:[24] $\sigma=0.340$ nm and $\varepsilon=167\times10^{-23}$ J. Using this value of ε, the relation expressing the absolute temperature versus reduced one is $T=121T^*$ [K].

Changes in the atom configurations were realized by the displacement of a randomly selected atom by a randomly chosen vector within a cube of edge length $2\Delta x$, where Δx is the maximum allowed displacement in one direction. The acceptation probability p of a new position of the atom is determined using the Metropolis criterion in the form

$$p=\exp(-\Delta U/k_BT), \tag{2}$$

where ΔU denotes the change in the interactions energy (equal to the difference between values of the energy in the starting and the final atom position) due to the analyzed displacement. When $\Delta U<0$, it is assumed that $p=1$ instead of calculating this value from Eq. (2). In every MC step, there were N_s attempts to displace an atom, each time randomly selected from N_s atoms in the system. Finally, what is typical for many simulations, the simulation cubic cell of edge length L was replicated in three dimensions to introduce periodic boundary condition.

In real conditions, a vapor is a reservoir of atoms enabling cluster growth by vapor condensation. In simulations of such a clustering process using the closed system—i.e., with a constant number of atoms in the simulation cell—the cluster growth would be accompanied by a steady decrease of vapor atoms. Simulations for the two-dimensional case reveal[25] that it is a time-consuming way for obtaining one cluster mainly due to the occurrence of a long period of Ostwald ripening. At that time, larger clusters grow by attachment of atoms evaporated from smaller ones. Our model is concentrated on growth simulations of the cluster which win in such a cluster-cluster competition. Therefore, only one central cluster, the nucleus, is selected to attach atoms from its neighborhood.

The cluster selection is realized by applying two different temperature regions in the simulation cell [Fig. 1(a)]. The temperature of surrounding vapor, T_v^*, should be chosen to be sufficiently high to avoid spurious nucleation—i.e., the formation of many small clusters inside the vapor and maintaining the vapor in an atomic state. For a high vapor temperature like $T_v=1.2$ of this work, the atom-atom interaction energy is relatively weak in comparison with the mean thermal energy k_BT. Consequently, the formation of stable bonds between vapor atoms is impossible. The situation is the opposite in the case of the nucleus, where the nucleus temperature T_n should be relatively low to enable atoms to join the cluster and nucleus. The value of T_n should be realistic and comparable with the cluster temperature if it is known from an experiment.

As shown in Fig. 1(a), the nucleus region of lower temperature is limited not only to the nucleus atoms but also contains a surrounding region extending up to R_{cl} from the nucleus atoms, where the parameter R_{cl} signifies the maximum allowed atom-cluster separation. This is strictly connected with the cluster determination method in the simulated system based on the geometrical criterion. During its random motion when an atom approaches another from the vapor or the nucleus at a distance less than R_{cl}, this atom is treated as part of a "temporary" vapor cluster or of the nucleus. A value of $R_{cl}=1.35$, approximately equal to the upper limit of the radius of the first coordination shell in a solid nucleus, was used in the simulations. An atom detachment from the nucleus to the vapor is also possible. It occurs when the atom displacement, proposed by the MC algorithm, leads to a point outside the nucleus region. When such an atom jump is accepted with probability p calculated from Eq. (2) for the nucleus temperature, the translated atom is treated in the next simulation steps to be vapor atom.

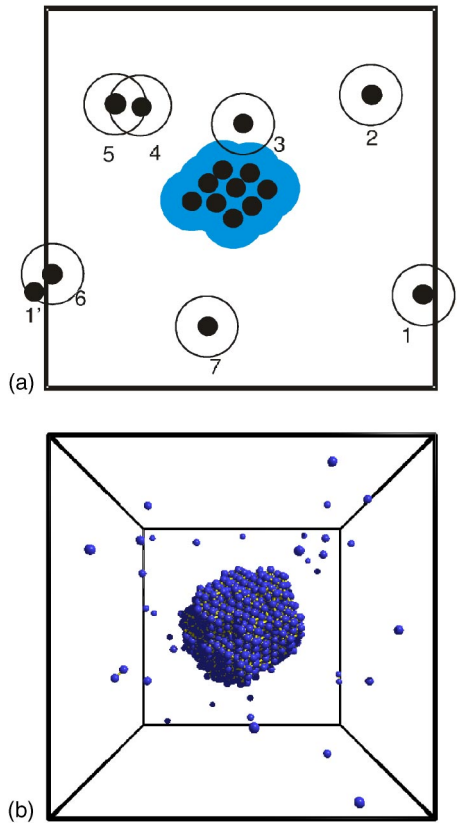

FIG. 1. (Color online) (a) Illustration of two regions, nucleus (gray/blue color) and vapor, in the simulation cell. If atoms in the system are at a distance less than R_{cl} (denoted by a circle around an atom), these atoms are treated as belonging to the same cluster. For example, vapor atoms 4 and 5 or 1′ and 6 form clusters, which are unstable due to the large vapor temperature. Atom 1′ is the image of atom 1 due to the implemented periodic boundary condition. (b) Typical view of the simulation cell during a simulation run with a growing cluster in the cell center and vapor atoms.

In the simulations the atom concentration n_v of vapor is kept constant, which is similar to the assumption of a constant atom flux in MD simulations.[20] This means that the attachment of atoms to the cluster must be connected with the addition of new atoms to the vapor region. This simple method to keep constant the vapor concentration by fixing the number of atoms in the simulation cell fails when the

cluster volume V_{cl} changes significantly in comparison with the simulation cell volume L^3. This is due to the large differences in atom concentration in the vapor n_v and in the cluster n_{cl}. One possible solution involving the enlargement of the simulation cell is inconvenient because this results in an increase in the number of vapor atoms and time-consuming translations of numerous vapor atoms. A better solution is to estimate from time to time, during simulations, the actual cluster volume V_{cl} and calculate the desired number of vapor atoms, N_v, from the simple relation

$$N_v = n_v(L^3 - V_{cl}). \tag{3}$$

In order to compute V_{cl} a simple procedure was used: (a) the cell is divided into many subcells, and (b) each subcell is proved to be a part of the cluster region resulting in *no* if it is separated more than of R_{cl} from all of the nucleus atoms. The nucleus atoms are identified much more often, which is done routinely in these simulations every 10 MC steps. An illustration of the spatial position of vapor atoms and the nucleus shape is given in Fig. 1(b).

III. DETERMINATION OF THE MODEL PARAMETERS

The two-temperature-region simulation model, as described above, requires seven parameters. However, only two of them—i.e., nucleus temperature T_n and vapor atom concentration n_v—are of great importance for determining the properties of a growing cluster and nucleus. The other five parameters expressed by the symbols R_{cl}, T_v, L, Δx_n, and Δx_v, though of lesser importance, are necessary to run the simulation program. The values of $R_{cl}=1.35$ and $T_v=1.2$ were justified in the previous section, while the motivation for the choice of the value of all remaining parameters is given below.

The nucleus temperature T_n should be related to the cluster temperature known from an experiment if one wants to explain the experimental results. Unfortunately, this parameter is seldom given in the literature in comparison with, for example, the cluster size or even with the predicted cluster structure. Depending on the experimental conditions and determination methods, slightly different cluster temperatures T_n have been reported: 35 ± 4 K (Ref. 6) and 37 ± 4 K (Ref. 26). On the other hand, in theoretical papers the reduced temperature T^* is used frequently instead of the temperature T. Ikeshoji *et al.*[14] analyzed cluster properties at the temperature $T^*=0.30$. This paper is devoted to a structure analysis of growing solid clusters. As is well known from the literature (e.g., see Ref. 27), the liquid-solid transition occurs at lower temperature for smaller cluster sizes. Therefore, for growth simulations three values of $T_n^*=0.25$, 0.30, and 0.35 ($T_n=30.3$ K, 36.3 K, and 42.4 K for argon clusters, respectively) were selected. At these temperatures the analyzed 201-atom cluster remains solid.[13,28]

It should be mentioned that in the initially fcc cluster [Fig. 2(a)] new local structures are developed when it is equilibrated at $T_n^*=0.30$ and 0.35 (cf. Ref. 13). As shown in Fig. 2(b) hcp layers are present at the cluster surface at $T_n^*=0.30$. Linear chains of units of noncrystalline decahedral (dh) local structure [called pentagonal direct-packed structure in Ref. 13 and shown there in Fig. 2(d)] in some clusters are also formed at $T_n^*=0.35$ [Fig. 2(c)]. These structural transformations in the seed cluster may have a great effect on the structure development during cluster growth. Therefore, it was decided to carry out ten simulations at the same growth conditions (n_v, T_n^*) but using ten different seed clusters, selected randomly among 17 obtained[13] in the heating-up process of the 201-atom cluster with an ideal fcc structure at $T^*=0$. The selected clusters were picked up from heating-up simulation data[13] at $T^*=0.25$, 0.29, and 0.35; therefore additional equilibration was needed only to increase the cluster temperature from $T^*=0.29$ to 0.30.

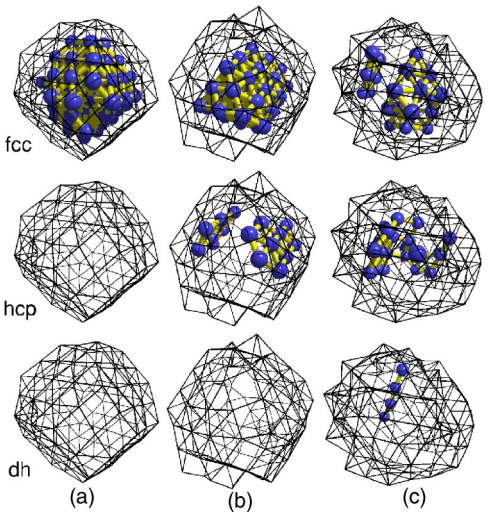

FIG. 2. (Color online) Arrangement of local structures in the 201-atom cluster equilibrated at three temperatures T_n^*: (a) 0.25, (b) 0.30, and (c) 0.35. The presentation of cluster structure is as follows: (i) dark/blue balls represent the local structure centers of a selected structure, (ii) light gray/yellow cylinders denote bonds between the centers, and (iii) surface net of dark thin cylinders linking the surface atoms marks the external shape of clusters.

In order to choose the optimal vapor concentration, the growth simulations of the 201-atom cluster were done with four values of n_v: 0.050, 0.010, 0.002, and 0.001. The value of the vapor concentration has a strong effect on the growth rate and the structural perfection of the clusters. In the case of lower vapor concentration the vapor atoms contact the nucleus more rarely during the same number of MC simulation steps. This results in slower cluster growth as measured by the number of MC steps needed to obtain the cluster of a given size. For example, at $T_n^*=0.25$ the averaged period of cluster growth from $N=201$ to $N\approx1650$ is 4447, 44 781, 250 250, and 519 646 (in MC steps) in the sequence of decreasing vapor concentration n_v, given above.

A larger number of simulation steps leads to a better cluster structure perfection [Fig. 3(a)] as measured by the order parameter F_o, which is defined as the ratio of the number of detected structural units per number N_{12} of atoms with completed 12 first neighbors [Fig. 3(b)]; for details, see Ref. 13. The cluster ordering reaches even 98% for $n_v=0.002$ and 0.001 and the cluster temperature $T_n^*=0.25$ and 0.30. The surprisingly low value of $F_o=91\%$ for $T_n^*=0.35$ can be explained by a partial destruction of the atom arrangement near

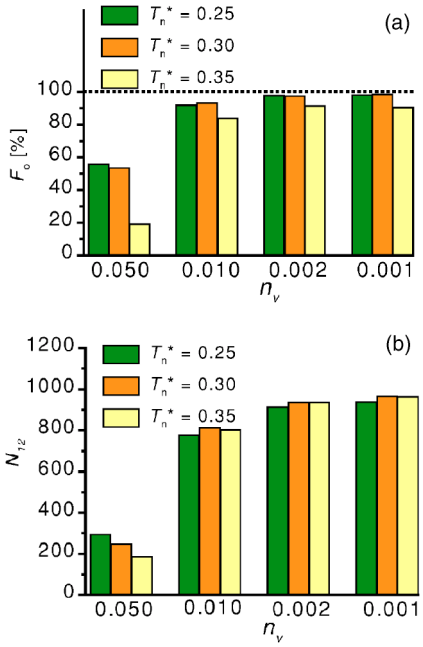

FIG. 3. (Color online) (a) Average cluster order parameter F_o calculated using ten clusters with $N \approx 1650$ obtained at the same vapor concentration n_v and the cluster temperature T_n^*. (b) Average number N_{12} of cluster atoms with the completed first coordination shell (12 atoms) up to the distance $R=1.35$. In (a) and (b) the structure analysis was limited to atoms added to the seed cluster LJ_{201}.

the cluster surface enabled by a high temperature. For comparison, the same process is already observed in the case of the equilibrated seed 201-atom cluster, where $F_o=96\%$, 95%, and 82% for $T_n^*=0.25$, 0.30, and 0.35, respectively.

As may be seen in Fig. 3(b) for $n_v=0.002$ and 0.001, the number N_{12} of atoms with completed first shell is practically the same at $T_n^*=0.30$ and 0.35. This means that, though some atoms near the surface lose the structure (evident from lower value of F_o) due to thermal vibration, clusters are still densely packed. This is intimately connected with changes in the cluster external shape (Fig. 4), where the clusters obtained at $n_v=0.002$ and 0.001 show a compact shape in comparison with those for $n_v=0.050$ and 0.010. The extremely high growth rate for $n_v=0.050$ leads to a ramified form of unstable clusters as shown in Fig. 4(a) with a highly disordered structure as can be deduced from Figs. 3(a) and 3(b). In our case, the cluster growth is too fast to enable sufficient cluster equilibration by the atom movement from the position of a lower atom bonding energy to that of a higher one, thereby leading to a destruction of cluster branches and attaining a more compact shape.

The high and similar values of F_o and N_{12} for clusters obtained at $n_v=0.002$ and 0.001 imply that both these values can be used alternatively in simulations. The choice of $n_v=0.001$ is optimal as far as the cluster structural perfection is concerned, but $n_v=0.002$ is also equally good especially when the scope of simulation is to obtain very large clusters during smaller computation time.

The vapor atom concentration n_v and the edge size L of the simulation cell determine the maximal number of vapor

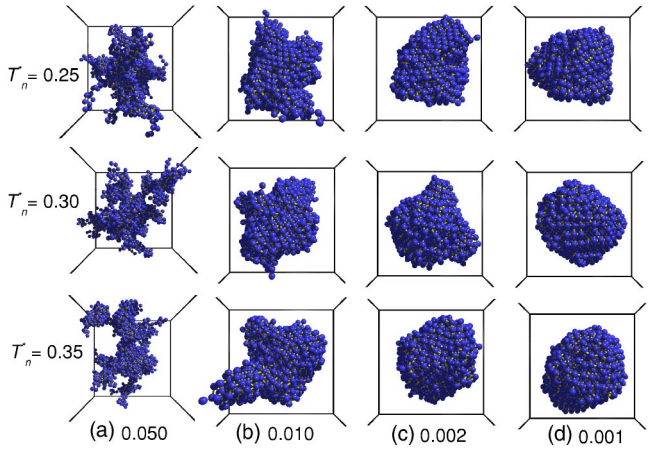

FIG. 4. (Color online) Changes in external shape of clusters with $N \approx 1650$ growing at different vapor concentration n_v and cluster temperature T_n^*. Vapor concentration n_v is given below each set of simulation. As seen in (c) and (d), a slower cluster growth leads to compact shapes.

atoms, N_v, in the system. Therefore, large L or large n_v results in a large number of vapor atoms. In some cases it could happen that N_v is greater than N even for sufficiently large cluster. This leads to an unnecessary increase in computation time, which is lost for the movement of numerous vapor atoms. The decrease of L also results in lower values of N_v. Unfortunately, for sufficiently small L (comparable with the cluster diameter) there appears a new obstacle: namely, the value of flux of randomly walking vapor atoms reaching the nucleus surface may depend on an analyzed position on the surface. For example, positions A and B in Fig. 5 are expected to be characterized by different atom flux because of the difference in the vapor width to neighboring nucleus image. Due to such geometrical reasons, the nucleus would have a tendency to grow faster towards the cell corners. In order to eliminate such an effect the value of $L=35.0$ was chosen, which denotes that the largest analyzed cluster with $N=2300$ atoms occupies merely 7.7% of the cell volume. The value of $L=35.0$ and the atom concentration

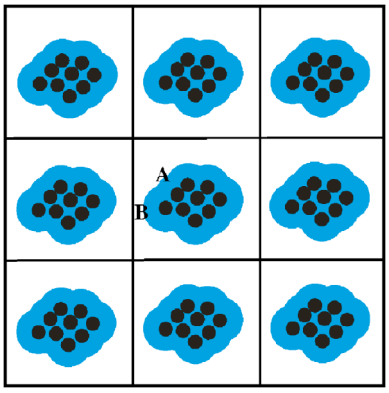

FIG. 5. (Color online) Realization of periodic boundary condition by multiplication of the simulation cell. Note that when the cell edge is too small (compared with cluster diameter), the atom flux reaching position B on the cluster surface is low in comparison with A due to location close to the cluster image (on the left vs B).

$n_v = 0.002$ lead to an acceptable value of $N_v = 86$ vapor atoms.

The value of the maximum allowed displacement Δx_n for the nucleus atoms was adjusted during the simulation run in order to keep the acceptance ratio close to 0.4 as is typically done in MC simulations. For the analyzed temperature $T_n^* = 0.30$ it resulted in $\Delta x_n \approx 0.13$. This value was proved to be too small for vapor atoms, which must walk (diffuse) a sufficiently long distance from a randomly chosen point in the vapor region (at the moment of atom addition to the system) to the nucleus, before their attachment. Moreover, due to the low density of vapor atoms and the high vapor temperature $T_v = 1.2$, practically all jumps are accepted irrespective of the chosen value of the maximum allowed displacement Δx_v of vapor atoms. Large values of Δx_v, leading to nonphysical trials of atom incorporation directly into the cluster interior, were excluded from the analysis. Finally, the value of $\Delta x_v = 5\Delta x_n$ was arbitrary chosen to be sufficiently large to reasonably decrease the number of steps in randomlike diffusion and sufficiently small to contact the walking atom with nucleus external atoms, thereby enabling its attachment solely to the nucleus surface.

IV. STRUCTURES IN GROWING CLUSTERS

Changes in the internal structure of the growing nucleus were monitored using the coordination polyhedron method[13] applied to *XYZ* data files corresponding to different nucleus sizes. If necessary, the obtained data of all local structures were used in a special program for the creation of input files for the graphics program POVRAY. The presentation of cluster structure is based on the following rules: (a) the local structure centers of a selected structure are dark (blue color in the online version of this paper) balls, (b) the centers are connected with bonds (light gray or yellow cylinders) if their distance is smaller than R_{cl}, and (c) surface net of dark thin cylinders, created by linking the surface atoms, marks the external shape of clusters.

There are many reports concentrated on finding the ideal cluster structure for a given N. Generally, these works did not take into account the possibility of defect formation. In fact, it is known[13] that perfect fcc 201-atom clusters may exist only at $T_n^* = 0.25$ due to the reported fcc to hcp surface transformation at $T_n^* = 0.29$. Therefore, when the acceptable values of n_v are selected (cf. Sec. III), the main task of further simulations is to know whether it is possible to grow a crystalline fcc cluster when the starting cluster is a perfect fcc one. In order to observe the influence of the structure transformation in the seed cluster on the growing cluster structure, two additional temperatures $T_n^* = 0.30$ and 0.35 were analyzed.

As discussed in the previous section, the vapor concentration has a strong influence on the cluster growth rate and the cluster structure perfection. The type of local structures is also concentration dependent. As shown in Fig. 6, for the highest analyzed concentration $n_v = 0.050$ some icosahedral centers are present (16 for $T_n^* = 0.25$). With decreasing n_v, the number of icosahedral local structures decreases, rapidly approaching zero. At the same time, a significant increase in the number of fcc and hcp structural units is observed,

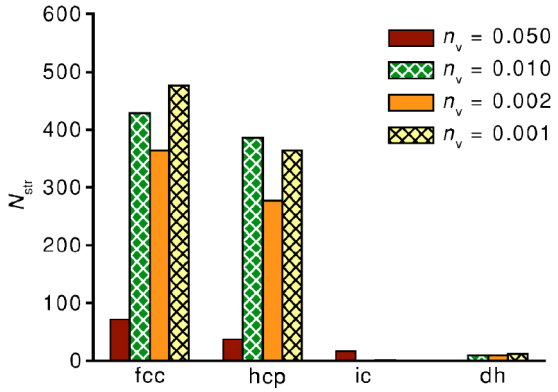

FIG. 6. (Color online) Average number N_{str} ($N_{str} = N_{fcc}$, N_{hcp}, N_{ic}, or N_{dh}) of investigated local structures in the nucleus composed of $N \approx 1650$ atoms shown for $T_n^* = 0.25$ and for different vapor concentrations n_v. The local structures present in the seed 201-atom cluster were excluded from statistics.

whereas the number of noncrystalline decahedral units is practically at the same level. Thus, the creation of hcp and dh structures is inseparably connected with the growth of fcc cluster structure.

After careful structure examination of all 60 clusters formed at the three investigated temperatures and the vapor concentration $n_v = 0.002$ and 0.001 it was found that most of the clusters (i.e., 53) show a regular internal structure. They may be grouped into six cluster structure types (Fig. 7): (a) column fcc, (b) tetrahedral fcc, (c) defective layered fcc/hcp, (d) layered fcc/hcp, (e) decahedral, and (f) polytetrahedral cluster. The remaining seven irregular clusters [Fig. 7(g)] were often observed at $T_n^* = 0.35$.

The cluster structures (a)–(f) are characterized by the presence of hcp layers which cross themselves at an angle close to $\alpha = 70.53°$ or $\beta = 109.47°$ or which are parallel [type (d)]. This is because they grow on an fcc core, where the angle between the dense-packed (111) planes can be α or β or equal to 0 for parallel layers. The formation of hcp layers

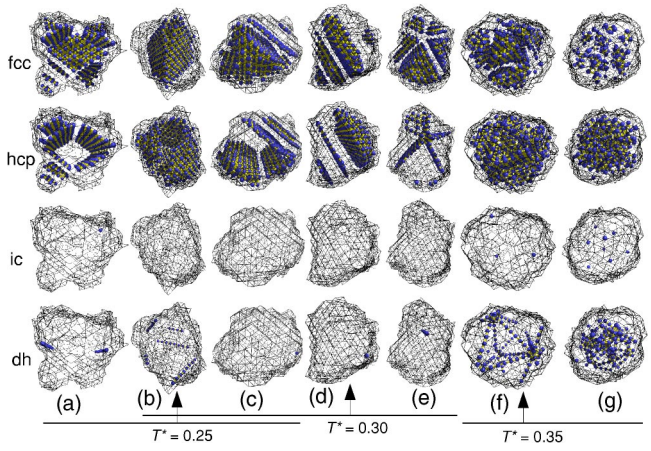

FIG. 7. (Color online) Typical internal structures observed among 60 clusters with $N \approx 1650$ atoms grown at $n_v = 0.002$ or 0.001: (a)–(f) regular and (g) irregular. Horizontal lines mark typical structures for a given temperature, while arrows indicate most frequently found clusters.

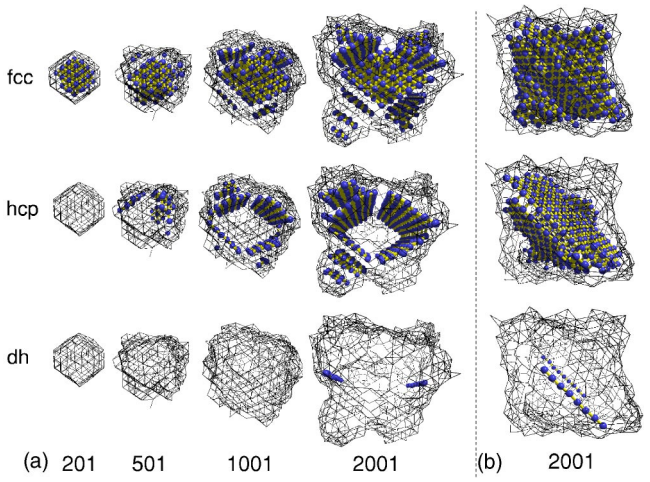

FIG. 8. (Color online) (a) Illustration of the crossing of hcp layers in a column fcc cluster leading to creation of two parallel dh linear chains with increasing N. (b) The cluster of (a) with $N=2001$ shown from another direction.

on some dense-packed fcc layers is due to a misfit in the position of newly added atoms resulting in a …*ABCABA* instead of …*ABCABC* layer sequence. Subsequent growth of this plane can lead to an enlargement of the hcp layer width or to the formation of a new fcc layer over the existing hcp layer, a process which can be called as kinetic trapping of hcp plane. The newly created fcc layer can also be trapped kinetically. Consequently, alternative hcp and fcc layers are often found in simulated clusters. This process is clearly illustrated in Fig. 8(a) for the growth of a column fcc cluster.

As observed in the simulations, two hcp planes crossing at an angle 70.53° usually form a linear chain of local dh structures characterized by a linear pentagonal symmetry in the contact region [Fig. 8(a) for $N=2001$]. This is a result of similar values of 70.53° and $72°=360°/5$ for pentagonal symmetry. This energetically favorable mechanism transforms a defected crystalline fcc/hcp [Fig. 7(c)] to a noncrystalline decahedral cluster [Fig. 7(e)] or produces dh chains in tetrahedral and polytetrahedral clusters [Figs. 7(b) and 7(f)]. It was found that the linear dh chains usually cross themselves [Fig. 7(f)]. However, among 60 clusters, 4 clusters characterized by two parallel dh chains were found [Fig. 8(b)]. van de Waal argued[12] that the existence of two parallel linear defects of pentagonal symmetry in the rare-gas clusters can lead to a solution of the RGS problem in terms of the growth kinetics of such defected clusters. However, here it should be emphasized that the creation of pairs of dh chains is a consequence of hcp formation during an atom-by-atom cluster growth of an fcc core, and not by coalescence or intergrowth of decahedral clusters as proposed by van de Waal.[12]

It was found during the simulations that typically the clusters grow without structural changes in the internal part of the cluster; i.e., structure formation occurs near the cluster surface during the addition of new atoms. However, one important exception was observed in case of the decahedral cluster shown in Fig. 7(e). Its growth history, illustrated in Fig. 9, reveals that very well arranged fcc and hcp layers

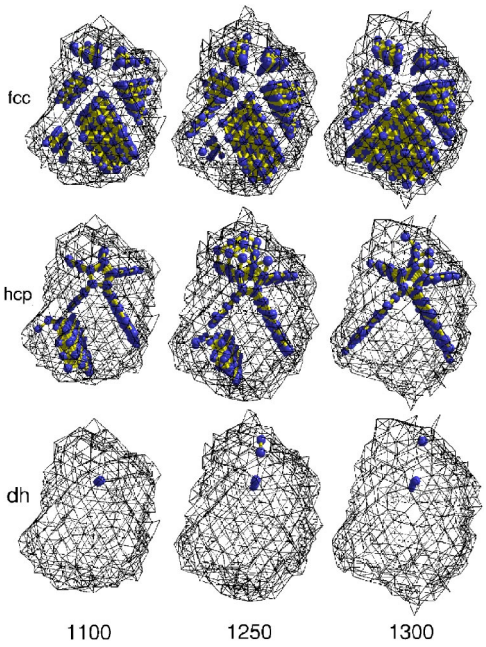

FIG. 9. (Color online) (a) Three snapshots showing structural rearrangement in cluster part, where initially two hcp layers cross themselves at the angle ca. 109.47°. After rearrangement at $1250<N<1300$, the cluster internal structure attains the structure of decahedron characterized by one line of dh units and five fcc sectors. The same cluster is also shown in Fig. 7(e) for $N=1650$.

were rearranged by destroying the spurious hcp layer, which contact with another hcp plane at an angle close to $\beta=109.47°$. In such a way, the fifth fcc sector emerges and the decahedral cluster is formed. Thus, this partial cluster structural transition is able to transform a crystalline or defected crystalline cluster to noncrystalline one of decahedral character.

V. CONCLUSIONS

The advantages of the cluster growth model proposed in this work are (i) randomlike motion of vapor atoms giving the same attachment probability irrespective of the angle between the atom flux and cluster surface and enabling analysis of ramified cluster shapes in the case of fast growth, (ii) possibility to overcome the time-consuming Ostwald ripening by applying a high temperature for the surroundings of a selected cluster, and (iii) effective growth simulation of small- or medium-sized clusters up to relatively large sizes. Using the present model, with the optimal vapor concentration $n_v=0.002$ reported in this work, it was recently found[29] that it is relatively easy to obtain in simulations on a workstation very large LJ clusters composed of $N=10\,000$ atoms.

Since this work is aimed at observing the structural evolution of a growing perfect fcc cluster, the maximal analyzed size is decided to be approximately 2000, because below this size the fcc structure in the seed cluster always changes to a mixture of generally three types of structures: fcc, hcp, and dh. Such structural transitions are attributed to three mechanisms. The first mechanism involves partial destruction of

the fcc structure in the seed cluster LJ_{201} caused by sufficiently high temperature (from $T_n^*=0.30$). The second is kinetic trapping of fcc and hcp dense-packed layers, leading to the formation of stacking faults. When kinetically trapped hcp planes cross themselves at an angle close to 70.53°, they form a linear chain of local dh structures coming through the entire cluster and characterized by a linear pentagonal symmetry. The third mechanism is an atom rearrangement in the cluster part, where two hcp planes contact themselves at the angle close to 109.47°. After this partial transformation only a pentagonal linear defect stays, giving the decahedral character to the entire cluster.

The creation of defected structures like clusters with two parallel linear defects of pentagonal symmetry, as observed during these simulations, supports van de Waal's arguments[12,15,16] that cluster defects play a decisive role in the explanation of the RGS problem. Experimental results[6,7] also reveal that defective clusters dominate the cluster spectrum until $N=10^5$, but their structure was not guessed during data analysis. The cluster structures, presented in this work, can be helpful in such predictions, because they were obtained in simulations at real temperatures. However, for the identification of an experimental cluster structure it is better to use a smaller cluster as the seed cluster instead of an arbitrarily chosen fcc LJ_{201}. The best candidate used in the simulations[30] is the icosahedral LJ_{13}, which is widely accepted in the literature to be formed during growth of a rare-gas clusters.

Finally, it should be stressed that the growth of a hypothetic fcc cluster unavoidably results in the formation of undesirable defects in the form of hcp and dh local structures. This implies that successful attempts to find an ideal fcc cluster, corresponding to the global minimum of cluster potential energy for a large number of cluster atoms, is not equivalent to the solution of the RGS problem.

ACKNOWLEDGMENTS

This work was financed by the State Committee for Scientific Research (Poland) through the research Project No. 2 P03B 027 25. The support by the computational grant KBN/-SGI_ORIGIN_2000/PLubelska/064/199 from ACK Cyfronet AGH (Cracow, Poland) is also acknowledged. The author expresses his gratitude to Professor K. Sangwal for encouragement during this work and to Dr. K. Wójcik for technical support.

[1] G. Torchet, M.-F. de Feraudy, A. Boutin, and A. H. Fuchs, J. Chem. Phys. **105**, 3671 (1996).
[2] R. Ahlrichs and C. Ochsenfeld, Ber. Bunsenges. Phys. Chem. **96**, 1287 (1992).
[3] F. Baletto, R. Ferrando, A. Fortunelli, F. Montalenti, and C. Mottet, J. Chem. Phys. **116**, 3856 (2002).
[4] J. P. K. Doye and F. Calvo, Phys. Rev. Lett. **86**, 3570 (2001).
[5] F. Baletto, C. Mottet, and R. Ferrando, Surf. Sci. **446**, 31 (2000).
[6] B. W. van de Waal, G. Torchet, and M.-F. de Feraudy, Chem. Phys. Lett. **331**, 57 (2000).
[7] M.-F. de Feraudy and G. Torchet, J. Cryst. Growth **217**, 449 (2000).
[8] K. F. Niebel and J. A. Venables, in *Rare Gas Solids*, edited by M. L. Klein and J. A. Venables (Academic Press, London, 1976), Vol. 1, Chap. 9.
[9] T. Kihara and S. Koba, J. Phys. Soc. Jpn. **7**, 348 (1952).
[10] F. H. Stillinger, J. Chem. Phys. **115**, 5208 (2001).
[11] J. P. J. M. van der Eerden, in *Crystal Growth—From Fundamentals to Technology*, edited by G. Müler, J.-J. Métois, and P. Rudolph (Elsevier, Amsterdam, 2004), pp. 190, 193, 194.
[12] B. W. van de Waal, J. Cryst. Growth **158**, 153 (1996).
[13] W. Polak and A. Patrykiejew, Phys. Rev. B **67**, 115402 (2003).
[14] T. Ikeshoji, G. Torchet, M.-F. de Feraudy, and K. Koga, Phys. Rev. E **63**, 031101 (2001).
[15] B. W. van de Waal, Phys. Rev. Lett. **67**, 3263 (1991).
[16] B. W. van de Waal, *The fcc/hcp Dilemma* (B. W. van de Waal, Twente, 1997).
[17] J. P. K. Doye, D. J. Wales, and R. S. Berry, J. Chem. Phys. **103**, 4234 (1995).
[18] L. T. Wille, in *Annual Reviews of Computational Physics VII*, edited by D. Stauffer (World Scientific, Singapore, 1999), pp. 25–60.
[19] R. S. Berry, J. Phys. Chem. **98**, 6910 (1994).
[20] F. Baletto, C. Mottet, and R. Ferrando, Phys. Rev. Lett. **84**, 5544 (2000).
[21] F. Baletto, J. P. K. Doye, and R. Ferrando, Phys. Rev. Lett. **88**, 075503 (2002).
[22] G. H. Gilmer, in *Facets of 40 Years of Crystal Growth*, edited by W. J. P. van Enckevort, H. L. M. Meekes, and J. W. M. van Kessel (University of Nijmegen, Nijmegen, 1997), pp. 6–7.
[23] M. Kotrla, Comput. Phys. Commun. **97**, 82 (1996).
[24] C. Kittel, *Introduction to Solid State Physics*, 5th ed. (Wiley, New York, 1976), Chap. 3.
[25] R. Mahnke, H. Urbschat, and A. Budde, Z. Phys. D: At., Mol. Clusters **20**, 399 (1991).
[26] E. T. Verkhovtseva, I. A. Gospodarev, A. V. Grishaev, S. I. Kovalenko, D. D. Solnyshkin, E. S. Syrkin, and S. B. Feodos'ev, Low Temp. Phys. **29**, 386 (2003).
[27] A. Rytkönen, S. Valkealahti, and M. Manninen, J. Chem. Phys. **108**, 5826 (1998).
[28] N. Quirke, Mol. Simul. **1**, 249 (1988).
[29] W. Polak (unpublished).
[30] W. Polak (unpublished).